

# Neuron Glia Biology

<http://journals.cambridge.org/NGB>

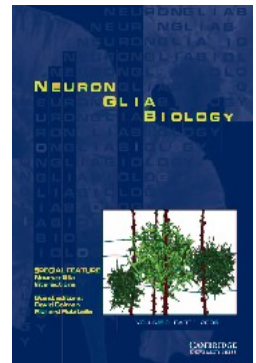
Additional services for *Neuron Glia Biology*:

Email alerts: [Click here](#)

Subscriptions: [Click here](#)

Commercial reprints: [Click here](#)

Terms of use : [Click here](#)



---

## Shapes of astrocyte networks in the juvenile brain

VANESSA HOUADES, NATHALIE ROUACH, PASCAL EZAN, FRANK KIRCHHOFF, ANNETTE KOULAKOFF and CHRISTIAN GIAUME

Neuron Glia Biology / Volume 2 / Issue 01 / February 2006, pp 3 - 14  
DOI: 10.1017/S1740925X06000081, Published online: 14 February 2006

**Link to this article:** [http://journals.cambridge.org/abstract\\_S1740925X06000081](http://journals.cambridge.org/abstract_S1740925X06000081)

### How to cite this article:

VANESSA HOUADES, NATHALIE ROUACH, PASCAL EZAN, FRANK KIRCHHOFF, ANNETTE KOULAKOFF and CHRISTIAN GIAUME (2006). Shapes of astrocyte networks in the juvenile brain. *Neuron Glia Biology*, 2, pp 3-14  
doi:10.1017/S1740925X06000081

**Request Permissions :** [Click here](#)

# Shapes of astrocyte networks in the juvenile brain

VANESSA HOUADES<sup>1</sup>

NATHALIE ROUACH<sup>1</sup>

PASCAL EZAN<sup>1</sup>

FRANK KIRCHHOFF<sup>2</sup>

ANNETTE KOULAKOFF<sup>1</sup>

AND

CHRISTIAN GIAUME<sup>1</sup>

*The high level of intercellular communication mediated by gap junctions between astrocytes indicates that, besides individual astrocytic domains, a second level of organization might exist for these glial cells as they form communicating networks. Therefore, the contribution of astrocytes to brain function should also be considered to result from coordinated groups of cells. To evaluate the shape and extent of these networks we have studied the expression of connexin 43, a major gap junction protein in astrocytes, and the intercellular diffusion of gap junction tracers in two structures of the developing brain, the hippocampus and the cerebral cortex. We report that the shape of astrocytic networks depends on their location within neuronal compartments in a defined brain structure. Interestingly, not all astrocytes are coupled, which indicates that connections within these networks are restricted. As gap junctional communication in astrocytes is reported to contribute to several glial functions, differences in the shape of astrocytic networks might have consequences on neuronal activity and survival.*

**Keywords:** Astrocytes, connexins, neuroglial interactions, intercellular communication

## INTRODUCTION

Although several reports indicate that there are subpopulations of astrocytes (Steinhauser *et al.*, 1992; Kressin *et al.*, 1995; Matthias *et al.*, 2003; Grass *et al.*, 2004; Wallraff *et al.*, 2004; Haas *et al.*, 2005; but see also Walz, 2000). However, a characteristic feature of most of them is the high level of gap junction expression, which provides a direct pathway for intercellular communication between astrocytes and, in some cases, between astrocytes and oligodendrocytes, as shown in co-cultures (Venance *et al.*, 1995) and in corpus callosum slices (V. Houades, unpublished) and between astrocytes and neurons (Nagy and Rash, 2000). Indeed, in the brain, astrocytes express the largest amount of connexins (Cx), the molecular constituents of gap junction channels. Gap junction channels consist of closely packed hemichannels formed by hexameric ring of Cxs that align head-to-head between neighboring cells to form functional intercellular channels. In mammalian brain at least eight Cxs have been identified, and Cx43 and Cx30 are the major Cxs detected in astrocytes (Nagy and Rash, 2000; Rouach *et al.*, 2002a; Theis *et al.*, 2005). In addition, although some studies show that expression of Cx26 is restricted to subpopulations of astrocytes (Mercier and Hatton, 2000; Nagy *et al.*, 2001), its expression in astrocytes is controversial (Filippov *et al.*, 2003). The expression of several Cxs in astrocytes might confer distinct properties to gap junction channels by providing differential regulation, gating and permeability. Finally, recent evidence indicates that Cx43 might also operate as hemichannels, allowing the release of ‘gliotransmitters’ from astrocytes (Bennett *et al.*, 2003; Ye *et al.*, 2003).

Initial studies related to the functional properties of astrocyte gap junctions have been performed in culture models

and in acute brain slices. In both cases, the widespread diffusion of intercellular tracers permeant to junctional channels (Lucifer yellow and biocytin) indicates that the level of gap junction-mediated intercellular communication is much greater between astrocytes than between either oligodendrocytes (Ransom and Yé, 2005) or neurons (Roerig and Feller, 2000). Such a high degree of intercellular communication has led to the proposition that astrocytes are organized in networks of communicating cells that might be subject to remodeling and plasticity (Giaume and McCarthy, 1996). Like other classes of ionic membrane channels, gap junction channels are regulated in two time scales: one, which represents long-term regulation (hours/days), operates at the levels of transcription, translation and degradation, and is associated with changes in the number of junctional channels; the other is a short-term regulation (minutes) consisting of changes in the biophysical properties (open probability, open time, unitary conductance and sub-conductance states) of junctional channels that are already present at gap junction plaques. This indicates that the extent of astrocytic networks is dynamic and can be controlled by several mechanisms acting through these two regulatory pathways. Interestingly, the expression of Cxs and gap junctional communication are targets for many endogenous active molecules such as neurotransmitters, growth factors, peptides, cytokines and endogenous bioactive lipids. This indicates that astrocytic networks are subject to plasticity, controlled by products secreted by neurons and by other cell types in the brain including astrocytes, microglial and endothelial cells (Rouach *et al.*, 2002a). In addition, gap junctional communication and Cx expression are modulated in astrocytes when they are cultured in the presence of several brain cell types, which has led to the concept that astrocyte gap

junctions represent a target for interglial and neuroglial interactions (Rouach *et al.*, 2000; Rouach *et al.*, 2002b; Faustmann *et al.*, 2003; Koulakoff *et al.*, 2003; Hinkerohe *et al.*, 2005). Finally, the expression of astrocytic Cxs is also affected in pathological situations that result from brain injuries and neurodegeneration (Rouach *et al.*, 2002a; Nakase and Naus, 2004). Together these findings indicate that Cx expression and astrocyte gap junctional communication (AGJC) are under the control of a broad spectrum of signals.

Evidence that is accumulating from neuroglial interaction studies confers new roles for astrocytes in neuronal activity and survival (reviewed in Ransom *et al.*, 2003). In this context, the participation of astrocytes in various brain functions should be also considered as the result of coordinated groups of communicating cells. We have, thus, performed an analysis of the shape of astrocytic networks in relation to the well-known neuronal organization in two brain structures, the hippocampus and the cerebral cortex. This study was performed at a defined age [postnatal days 9 to 11 (P9–P11)], when Cx43 is the major Cx expressed in astrocytes (Cx30 appears after the second postnatal week) (Kunzelmann *et al.*, 1999). Here, we report that, in addition to cellular domains defined by the morphology of single astrocytes, the presence of many gap junctions sets a second level of organization for astrocytes, termed astrocytic network. These networks, which are based on gap junction-mediated intercellular communication, involve several tens of cells, and their spatial organization depends on their location within defined brain structures.

## OBJECTIVE

The present study was designed to gain insight into the organization of astrocytic networks in two brain structures, the cerebral cortex and the hippocampus, in which the neuronal organization is well-established. This was achieved using two approaches: (1) analyzing the distribution of astrocytic connexins, the molecular constituents of gap junction channels, by immunofluorescence/confocal microscopy; and (2) determining their functional status by analyzing the shape and the extent of intercellular diffusion of two gap junction-permeable tracers in acute brain slices.

## MATERIALS AND METHODS

All experiments involving animals were carried out in accordance with the European Community Council Directives of November 24th 1986 (86/609/EEC) and all efforts made to minimize the number of animals used and their suffering. Experiments conformed to INSERM guidelines. Slices and sections were prepared from OF1 mice (Charles River). Transgenic (FVB/N) mice with fluorescent astrocytes expressing EGFP under the control of the human GFAP promoter were also used (Nolte *et al.*, 2001; Hirrlinger *et al.*, 2004).

### Tissue preparation and immunofluorescence labeling

P11 mice were anesthetized, perfused with phosphate-buffered saline (PBS) and their brains were removed rapidly and frozen in isopentane cooled at  $-30^{\circ}\text{C}$ . Coronal sections ( $20\ \mu\text{m}$ ) were cut on a cryostat, collected on slides and kept at  $-80^{\circ}\text{C}$

until use. Sections through the cortex and the hippocampus of mice were fixed with 2% paraformaldehyde in PBS for 30 minutes at  $4^{\circ}\text{C}$ , washed 3 times with PBS and preincubated 30 minutes in PBS containing 0.2% gelatin and 0.2% Triton-X100 (PBS\*). Sections were then processed for immunohistochemical staining by overnight incubation at  $4^{\circ}\text{C}$  with primary antibodies diluted in PBS\*. Antibodies used: mouse anti-Cx43 mAb (1:500, BD Bioscience); rabbit anti-GFAP (1:1000, Sigma); and mouse anti-NeuN mAb (1:500, Chemicon). After 3 washes, slices were incubated for 2 hours at room temperature with the appropriate secondary antibody, including TRITC-conjugated goat anti-mouse IgG (1:200) and FITC-conjugated goat anti-rabbit IgG (1:500, Southern Biotech). After several washes, slices were mounted in Fluoromount and examined with a microscope equipped with epifluorescence (Eclipse E800, Nikon). Images were acquired with a CCD camera coupled to image-analyzer software (Lucia, Nikon). Alternatively, a confocal laser-scanning microscope (Leica TBCS SP2) was used to visualize double immunostainings at high magnifications with  $63\times$  and  $100\times$  objectives; stacks of consecutive confocal images taken at 500 nm intervals were acquired sequentially with two lasers (argon 488 nm and helium/neon 543 nm) and Z projections reconstructed using Leica Confocal Software. Images covering large areas were obtained by assembly of several images captured with a  $10\times$  objective using the photomerge function of Adobe Photoshop software.

### Electrophysiology

P9–P11 mice were decapitated, their brains were dissected and placed in ice-cold artificial cerebrospinal fluid (ACSF) containing (in mM): 125 NaCl, 2.5 KCl, 25 glucose, 25 NaHCO<sub>3</sub>, 1.25 NaH<sub>2</sub>PO<sub>4</sub>, 2 CaCl<sub>2</sub>, and 1 MgCl<sub>2</sub>, bubbled with 95% O<sub>2</sub>;5% CO<sub>2</sub> (pH 7.4). Coronal brain slices ( $300\ \mu\text{m}$ ) containing the cerebral cortex and the hippocampus were cut using a vibratome (Leica, VT 1000GS) filled with ice-cold ACSF. The slices were transferred at  $34^{\circ}\text{C}$  for 1 hour before use. Thereafter, the slices were placed in a recording chamber under an upright microscope (Axioskop, Zeiss) and perfused continuously with oxygenated external solution (pH 7.4) at  $2\ \text{ml}\ \text{min}^{-1}$ . All experiments were carried out at room temperature ( $20\text{--}22^{\circ}\text{C}$ ). Cells in the CA1 area of the hippocampus and in the cerebral cortex were identified as astrocytes based initially on morphological criteria, using either infrared-differential interference contrast microscopy or epifluorescence for EGFP reactivity in transgenic mice, and secondly on electrophysiological properties. The pipette ( $10\text{--}15\ \text{M}\Omega$ ) solution contained (in mM): 105 K-Gluconate, 30 KCl, 10 Hepes, 10 phospho-creatine Tris, 4 ATP-Mg<sup>2+</sup>, 0.3 GTP-Tris, and either 0.3 EGTA (adjusted to pH 7.3 with KOH). Biocytin ( $3\text{--}4\ \text{mg}\ \text{ml}^{-1}$ , Sigma) or sulforhodamine B ( $1\ \text{mg}\ \text{ml}^{-1}$ , Sigma) were added to the pipette solution before each experiment. Patch-clamp recordings, 5 kHz sampling and 3 kHz filtering, were performed with an EPC9/2 (HEKA Elektronik) in either current-clamp or voltage-clamp modes. Series resistances were compensated at 80%. The data were analyzed with Igor software. Input resistance ( $R_{\text{in}}$ ) was measured in voltage-clamp mode by applying hyperpolarizing voltage pulses ( $10\ \text{mV}$ ,  $100\ \text{msec}$ ) from a holding potential of  $-80\ \text{mV}$ . Biocytin and sulforhodamine B were allowed to diffuse passively for 20 minutes in current-clamp mode, after which the slice was immediately fixed.

## Intercellular diffusion and GJC quantification in brain slices

Brain slices were fixed at 4°C for at least 12 hours in PBS (pH 7.4) containing 4% paraformaldehyde. Biocytin revelation was performed by incubating the slices in either avidin-biotinylated horseradish peroxidase (ABC-Elite), reacting with 3,3-diaminobenzidine (DAB) as a chromogen. Slices were then embedded in Moviol and mounted on slides. Quantification of AGJC was achieved by measuring the diameter of biocytin diffusion (taken as the distance measured between the two extreme stained cell bodies) in the slices according to the perpendicular and parallel axes to the surface of the cortex or to the hippocampal CA1 pyramidal cell body layer. The intercellular diffusion of sulforhodamine B was captured on-line with a digital camera (Nikon D70) and analyzed with a PC computer.

## Statistical analysis

For each data group, results are expressed as mean  $\pm$  SEM, and  $n$  is the number of independent experiments. For statistical analysis of the  $x/y$  ratio, the resting membrane potential and the input resistance, a one-way ANOVA followed by

a Kruskal-Wallis test was used. An unpaired  $t$ -test was applied to compare the effect of carbenoxolone to the control. Differences are considered significant at  $P < 0.05$  (\*) and  $P < 0.01$  (\*\*).

## RESULTS

### Expression of Cx43 in the cerebral cortex and hippocampus of P11 mice

At this developmental stage considered, astrocytic gap junctions are composed mainly of Cx43, whereas Cx30, the other major Cx expressed in more mature astrocytes, is only detected in meningeal cells of the brain parenchyma. Accordingly, the distribution of Cx43 was examined in frontal sections through the cerebral cortex and the hippocampus of P11 mice. Double staining was achieved to visualize astrocytes by GFAP and to localize the expression of Cx43. GFAP immunoreactivity was lower in the cortex compared with the hippocampus. Moreover, NeuN staining, a specific marker of neuronal nuclei, was also performed to localize the different neuronal layers (Fig. 1A,B) in both areas.

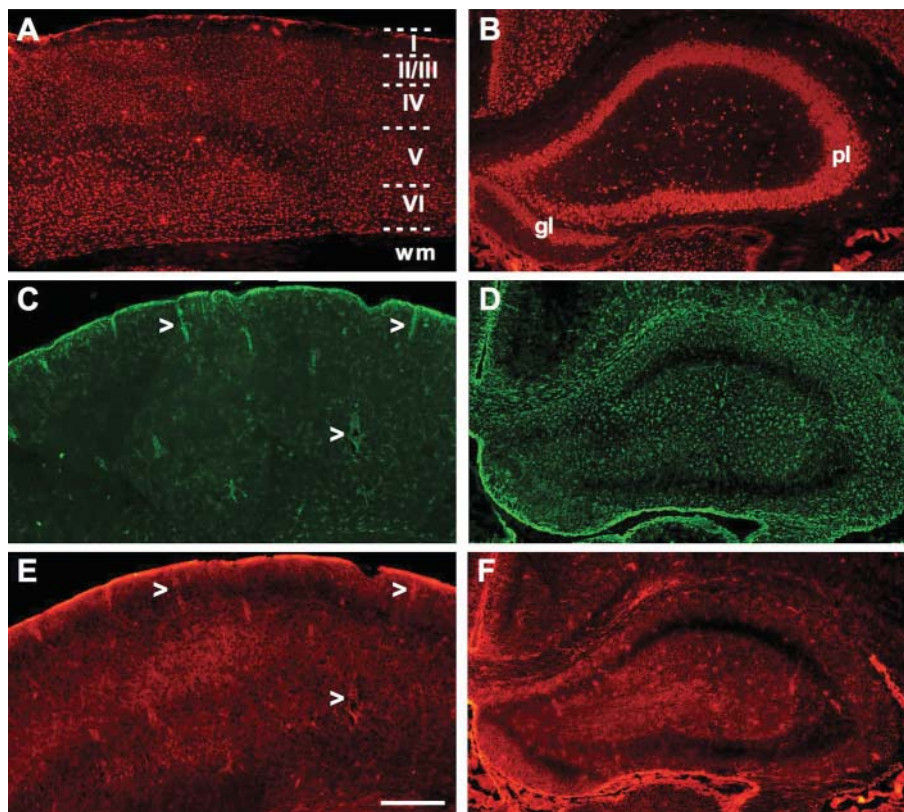


**Fig. 1. Expression of GFAP, NeuN and Cx43 in the cortex and the hippocampus at P11.** Immunofluorescence-labeling patterns in frontal sections at P11 with antibodies against astrocytic and neuronal markers (GFAP and NeuN, respectively), and against Cx43 in the mouse cerebral cortex (left) and the hippocampus (right). (A,B) NeuN staining shows the organization of neurons in layers in the cortex (A), from superficial layer I below the meninges to layer VI above the white matter (wm), and in the hippocampus (B) (pl indicates the pyramidal layer and gl the granule cell layer of the dentate gyrus). (C–F) Double staining for GFAP (C,D) and Cx43 (E,F) of sections through the cerebral cortex (C,E) and the hippocampus (D,F). Note in the cortex the laminar distribution of Cx43 and the brighter staining associated with blood vessels (arrowheads), whereas GFAP immunoreactivity, which is strong in the glia limitans and around blood vessels, is poorly detectable in cortical parenchyma. In the hippocampus, Cx43 expression is low in neuronal layers compared with that in astrocytes that are brightly stained with GFAP in stratum oriens and stratum radiatum. Scale bar, 250  $\mu$ m.

### Cerebral cortex

GFAP staining did not show a laminar distribution in the cortex but the onset of a laminar distribution was detected for Cx43 (Fig. 1C,E). Indeed, regions enriched in Cx43 were observed, particularly in the superficial layer I below the brightly stained meninges and in the deep layers IV and VI, whereas expression was lower in layer II/III and part of layer V (Fig. 1E). Bright staining of Cx43 was also present around blood vessels that were detected by GFAP labeling of astrocytic end-feet (Fig. 1C,E, arrowheads).

### Hippocampus

In the hippocampal formation, the distribution of Cx43 was clearly defined in regards to neuronal location. Weak staining for Cx43 was observed at the level of the pyramidal cell body layer and of the granule cells in the dentate gyrus compared with strong labeling in astrocytes from stratum oriens and stratum radiatum (Fig. 1D,F). At higher magnification, few puncta of Cx43 were detected in astrocytic processes crossing the pyramidal layer, but their density was higher in astrocytes of the surrounding tissue (Fig. 2A,B). Such low level of Cx43 expression correlates with the presence of only a few astrocytes inserted between pyramidal neurons and with elongated and reduced number of GFAP stained processes (Fig. 2B). However, spots of high Cx43 expression were detected on astrocytic end-feet that enwrap blood vessels (Fig. 2B, arrowhead). Interestingly, in stratum radiatum and oriens, a patchy distribution of Cx43 was detected, which indicates that expression of Cx43 is probably associated with domains that reflect territories occupied by the processes of single astrocytes (Fig. 2C,D). Such territories are poorly visible after immunostaining for endogenous GFAP. They are better revealed using preparations from GFAP-EGFP mice, which allow the visualization of the full cell bodies and all the dense ramifications made by astrocytic processes (Fig. 2E). In addition, expression of Cx43 is not higher at putative sites of contact between adjacent astrocytes (Fig. 2F). At this developmental stage, the level of Cx43 is not homogeneous and significant differences are observed between domains of neighboring astrocytes (Fig. 2F).

## Electrophysiological properties of hippocampal and cortical astrocytes

Astrocytes were selected initially by morphological criteria such as the small size of their cell body and the emergence of several processes. Their identity was confirmed by electrical membrane properties (highly negative membrane potential  $-85 \pm 1$  mV,  $n = 60$  and  $-84 \pm 1$  mV,  $n = 23$ , and low input resistance  $29.4 \pm 2.1$  M $\Omega$ ,  $n = 54$  and  $38.6 \pm 7.0$  M $\Omega$ ,  $n = 10$  for the cortex and the hippocampus, respectively) and the lack of action potentials in response to depolarization. Recordings in current- and voltage-clamp modes (Fig. 3A<sub>1</sub>,A<sub>2</sub>) indicate that all the cells recorded in this study (60 and 23 for the cortex and the hippocampus, respectively) have a linear I/V relationship (Fig. 3B,C), and are defined as 'passive' astrocytes based on the classification established previously (Matthias *et al.*, 2003; Blomstrand *et al.*, 2004). During 20 minutes of whole-cell recording, which enabled the dialysis and intercellular diffusion of biocytin, the membrane potential remained stable, in a range of  $\pm 2$  mV, and the linear I/V relationship was observed continuously.

## Intercellular diffusion of biocytin in the cerebral cortex and in the hippocampus

The data presented here were obtained from 72 recorded cells, identified as astrocytes following the criteria indicated above, of which 69 were coupled by gap junctions based on intercellular diffusion of biocytin.

### Cerebral cortex

As illustrated in Fig. 4, biocytin injections carried out by dialysis of an astrocyte during whole-cell recording were performed in four layers of the cerebral cortex. Intercellular diffusion of the tracer resulted in the staining of numbers of neighboring cells. The averaged numbers of coupled cells are:  $75 \pm 14$  ( $n = 9$ ) for layer I,  $73 \pm 15$  ( $n = 11$ ) for layer II/III,  $61 \pm 14$  ( $n = 10$ ) for layer IV and  $59 \pm 9$  ( $n = 8$ ) for layer V. These numbers are not statistically different, indicating that the amount of intercellular communication between astrocytes is similar in all cortical layers. Although differences in the density of receiving cells in the different cortical layers cannot be excluded, the area of coupling is not statistically different. By contrast, a difference is observed when considering the spatial organization of these coupled cells. To quantify this, the relationship between the distances of diffusion measured according to the axes perpendicular (Y) and parallel (X) to the surface of the cortex was taken as an index for the spatial organization of the coupled cells. The X:Y ratios were  $1.54 \pm 0.04$  ( $n = 9$ ) for layer I,  $1.40 \pm 0.03$  ( $n = 11$ ) for layer II/III,  $1.00 \pm 0.02$  ( $n = 10$ ) for layer IV and  $0.99 \pm 0.02$  ( $n = 8$ ) for layer V. This indicates that the intercellular diffusion of biocytin was circular in the two deeper layers but extended in the transversal direction in layers I and II/III. These differences are apparent from plotting the regression line for these two parameters because they are located on the bisector for layers IV and V (Fig. 4A<sub>1</sub>,B<sub>1</sub>) and are statistically distinct from this line in the upper layers close to the surface (Fig. 4C<sub>1</sub>,D<sub>1</sub>). Interestingly, in all the injections performed in an astrocyte located in layer I ( $n = 9$ ), a linear row of cells was also stained by biocytin, that corresponded to a heterotypic coupling between astrocytes and cells forming the glia limitans (Fig. 6A<sub>1</sub>,A<sub>2</sub>).

### CA1 hippocampal region

In this area, patch-clamp recordings and biocytin injections were performed in two locations of the stratum radiatum: either in the middle of this hippocampal area (Fig. 5A<sub>1</sub>,A<sub>2</sub>) or in the vicinity ( $<50$   $\mu$ m) of the pyramidal cell body layer (Fig. 5B<sub>1</sub>,C<sub>2</sub>). In these experiments, there were no significant differences in the number of coupled cells after injections into these two hippocampal regions,  $83 \pm 9$  ( $n = 13$ ) and  $71 \pm 10$  ( $n = 6$ ), respectively. The X and Y axes were taken as parallel and perpendicular to this neuronal layer, respectively. When biocytin injections were performed in an astrocyte located in the center of the stratum radiatum (Fig. 6B), the diffusion area was circular with an averaged X:Y ratio of  $0.96 \pm 0.01$  ( $n = 6$ ). In contrast, this relationship was  $1.39 \pm 0.07$  ( $n = 13$ ) following injection into the stratum radiatum close to the pyramidal cell body layer ( $<50$   $\mu$ m) (Fig. 5, left). Moreover, the latter injections distinguished two types of network shapes. In seven cases, dialysis of an astrocyte did not cause staining of astrocytes in the stratum oriens (i.e. on the other side of the pyramidal layer) (Fig. 5B<sub>1</sub>,B<sub>2</sub>). However, in six cases, the diffusion of biocytin also occurred in cells located in the stratum oriens

(Fig. 5C<sub>1</sub>,C<sub>2</sub>). It is noteworthy that the biocytin-positive cells either in or close to the pyramidal cell layer are distinct from neuronal cells: they had a bipolar and elongated morphology (Fig. 6C) that corresponded to astrocytes observed in this location with either GFAP staining (Fig. 2B) or with GFAP-EGFP (not illustrated). Finally, the number of coupled cells was not statistically different in the three situations described above (Fig. 5, right).

In both cortical and hippocampal structures, perfusion of the slices with carbenoxolone (100  $\mu$ M), added 15 minutes before whole-cell recording, resulted in a large decrease in the number of coupled cells by 85% and 81% in the cortex and the stratum radiatum area of the hippocampus ( $11 \pm 1$ ,  $n = 8$  and  $9 \pm 1$ ,  $n = 4$ ), respectively. The inhibitory effect of this uncoupling agent demonstrates that the biocytin intercellular diffusion is mediated by gap junctions.

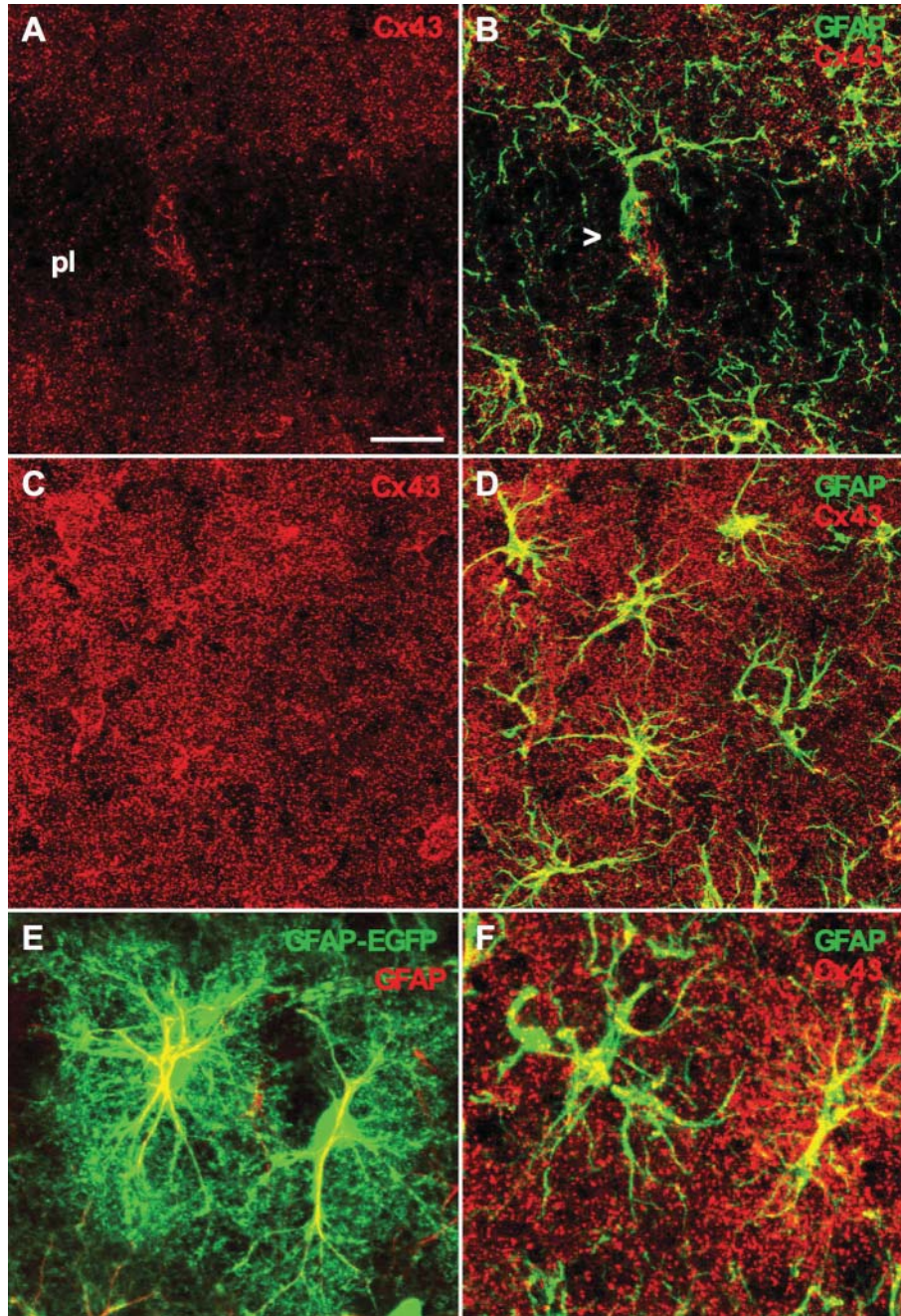


**Fig. 2. Confocal images of Cx43 distribution in astrocytes from the hippocampus (P11) identified by GFAP expression.** (A,B) Note the low density of immunoreactive Cx43 puncti that are associated with astrocytic processes crossing the pyramidal layer (pl), except at the level of GFAP positive end-feet enwrapping a blood vessel. (C,D) High density of Cx43 puncti in astrocytes from stratum radiatum. (E,F) Micrographs showing higher magnification of two astrocytes from GFAP-EGFP mice stained for endogenous GFAP in red (E) and wild-type mice doubly labeled for Cx43 and GFAP (F). Extensive branching of the processes that emanate from the two astrocytic soma is visible because of the cytoplasmic expression of EGFP, but is not detected fully by GFAP-antibody staining (E). Cx43-immunoreactive dots are distributed in the territory occupied by each astrocyte, not only at their edges (F). Scale bar: 20  $\mu$ m in A–D; 10  $\mu$ m in E,F.

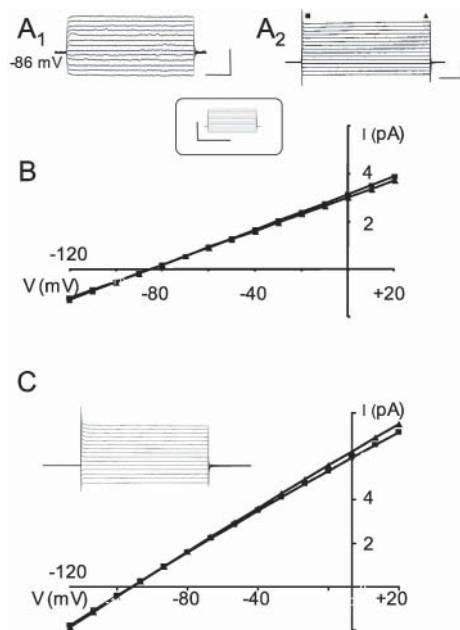


**Fig. 3. Electrophysiological properties of coupled astrocytes recorded from hippocampal and cortical slices.** (A<sub>1</sub>–A<sub>2</sub>) Recordings in voltage-clamp (A<sub>1</sub>) and current-clamp (A<sub>2</sub>) modes obtained from a hippocampal astrocyte coupled to 81 neighboring cells. Calibration bars: 2 nA and 25 ms for A<sub>1</sub>, and 20 mV and 100 ms for A<sub>2</sub>. The insert represents the pulse protocol used for voltage-clamp recordings, 100 mV and 100 ms. (B) Typical passive I/V relationship plotted from the values recorded in A<sub>1</sub>. (C) I/V relationship of a cortical astrocyte recorded in layer II/III that was coupled to 128 neighboring cells. Calibration bars: 2 nA and 30 ms, 20 mV and 100 ms.

### Dye coupling studied in GFAP–EGFP mice

In the structures mentioned above, recorded astrocytes filled with biocytin were coupled to cells that showed a similar morphology that is characteristic of astrocytes. Indeed, dye coupled cells never displayed a morphology that is typical of neurons and oligodendrocytes. To get more information on the phenotype of the cells that are coupled to the identified astrocytes, dye-coupling experiments were carried out using mice expressing EGFP under the GFAP promoter and using sulforhodamine B, rather than biocytin, as an intercellular tracer.

As reported for other brain areas, except for Bergmann glial cells in the cerebellum, confocal analysis of the double staining in hippocampus and the cortex confirmed the lack of a complete overlap between GFAP immunostaining and EGFP expression in slices from GFAP–EGFP transgenic mice (Nolte *et al.*, 2001). Indeed, in the hippocampus, staining with the anti-GFAP antibody resulted in a bright, filamentous staining that is typical of a cytoskeletal protein, whereas EGFP displayed a bright, diffuse green staining that is distributed evenly in the cell body and extensive arborizations of astrocytic processes (Fig. 7A). Moreover, although some of the stained cells were both GFAP- and EGFP-positive, many cells stained for either one or the other. This feature was more pronounced in the cortex because of the lower, less dense immunoreactivity of astrocytes for GFAP.

The level of AGJC was tested with sulforhodamine B, another intracellular tracer of gap junctions, which was selected because its emission spectrum is compatible with EGFP fluorescence. Using sulforhodamine B, the number of coupled cells was reduced significantly compared with

biocytin:  $36 \pm 14$  ( $n = 10$ ) versus  $59 \pm 10$  ( $n = 13$ ) in the hippocampus, and  $12 \pm 1$  ( $n = 15$ ) versus  $61 \pm 14$  ( $n = 10$ ) in the cortex. This is likely to be attributable to differences in the molecular weight of these two gap junction channel permeant molecules (biocytin, 378 Da and sulforhodamine B, 558 Da) and to differences in the treatment of the slices, which were fixed and revealed *a posteriori* for biocytin, and analyzed on-line from living slices for sulforhodamine B. In addition, there was no statistical difference ( $P > 0.1$ ) in the number of coupled cells studied with sulforhodamines in the cortex of OF1 and GFAP-EGFP mice ( $21 \pm 5$ ,  $n = 5$  and  $31 \pm 7$ ,  $n = 7$ , respectively). Confocal analysis of overlaid images indicates that  $49 \pm 9\%$  ( $n = 6$ ) and  $60\%$  ( $n = 2$ ) of sulforhodamine B-positive cells are also EGFP-positive in the hippocampus and the cortex, respectively (Fig. 7B arrows). Moreover, a significant number of green cells within the field of intercellular diffusion are negative for the gap junction tracer, which indicates that the astrocytic network revealed by dye coupling does not involve all the EGFP-positive cells in a defined area (Fig. 7B, arrowheads). However, in the present study we have not discriminated fully between weakly and strongly fluorescent EGFP cells that might distinguish between R-type and T-type sub-populations of astrocytes, as recently proposed (Matthias *et al.*, 2003).

### CONCLUSIONS

- The expression of Cx43 in astrocytes is not homogeneous in the cerebral cortex and the hippocampus of juvenile mice. Differences in expression are also detected between neighboring astrocytes.
- Most Cx43 immunoreactivity is not located at the area of contact between astrocytes.
- In both brain structures, gap junction-mediated intercellular communication involves  $>50$  cells, defining astrocytic ‘networks’.
- In addition to the notion of individual domains, communicating networks have to be considered as a second level of organization for astrocytes.
- In a defined area, not all astrocytes are coupled, which indicates astrocytic heterogeneity.
- The shape of these astrocytic networks depends on their location within neuronal compartments.

### DISCUSSION

The pattern of Cx43 expression and the level of AGJC were analyzed in parallel using immunofluorescence and confocal microscopy, and electrophysiological recordings in acute brain slices in juvenile mice at P9–11. Although older ages and adults remain to be investigated, our findings identify rules that account for the shape of the astrocytic network organization and we propose concepts that integrate this astrocytic property in the dynamic interactions between these glial cells and neurons.

### What dye coupling tells us about the functional status of gap junctions

There are multiple ways to assess the level of gap junctional communication between cells: (1) electrophysiological recordings of junctional ionic currents (Van Rijen *et al.*, 2001); (2)

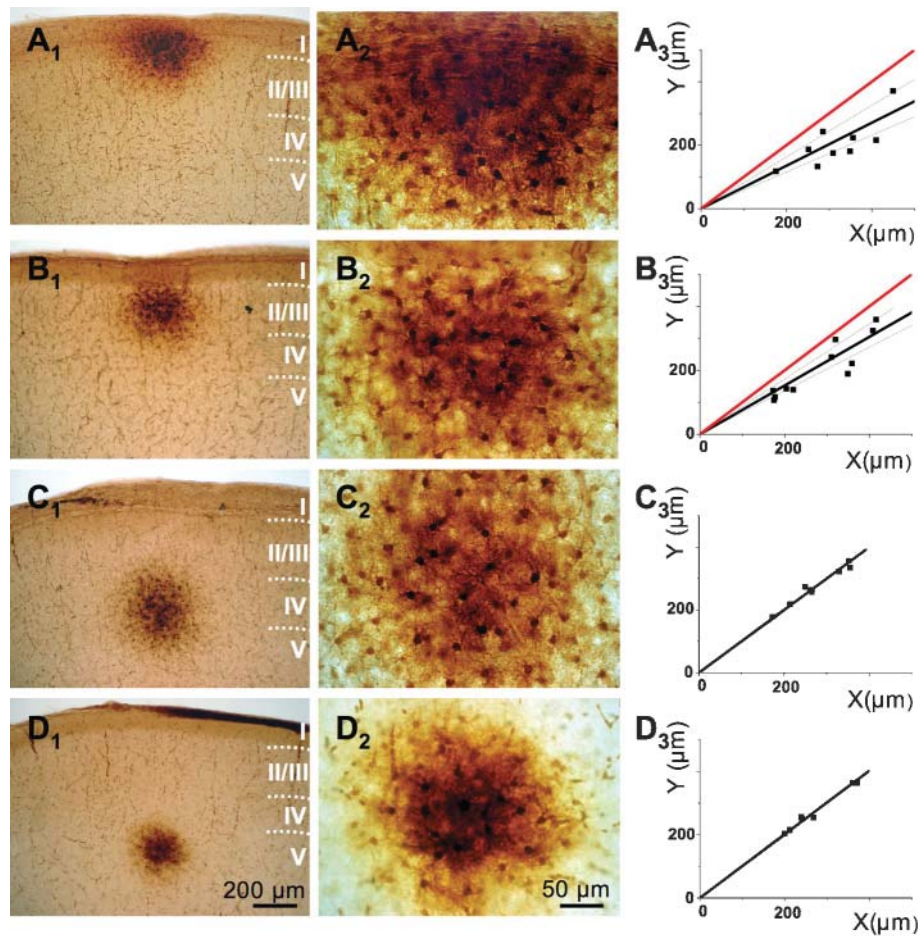


**Fig. 4. Astrocytic networks and intercellular diffusion of biocytin in the layers of the cerebral cortex.** Astrocytes, identified on morphological and electrophysiological bases, were filled with biocytin. The area of the spread of biocytin was compared with the location of the recorded cell in several cortical layers I (A<sub>1</sub>–A<sub>3</sub>), II/III (B<sub>1</sub>–B<sub>3</sub>), IV (C<sub>1</sub>–C<sub>3</sub>) and V (D<sub>1</sub>–D<sub>3</sub>), which were determined by anatomical analysis of neuronal distribution. Note that in layers I, II/III and IV, the number of coupled cells in the experiments illustrated is higher than the averaged number in the Results section and is identical for layer V ( $n = 58$ ). The shape of the coupling was analyzed according to two axes, parallel (X) and perpendicular (Y) to the surface of the cortex. The plot of regression lines and the confidence intervals indicate that coupling is circular in deep layers but oriented more in the transversal direction in layer I and II/III (A<sub>3</sub>–D<sub>3</sub>). Each square represents the quantification of a single injection and when the X:Y ratio differs from 1, the bisector (red line) is drawn for comparison. The correlation coefficients are 0.79 (layer I), 0.91 (layer II/III), 0.98 (layer IV) and 0.99 (layer V).

determination of dye coupling, which reflects the permeability of junctional channels for small dye molecules that can be visualized by histological techniques directly or after fixation (Méda, 2001); (3) intercellular calcium imaging and flash photolysis of caged compounds (Leybaert and Sanderson, 2001); and (4) imaging techniques based on either recovery after photobleaching (FRAP) or local activation (LAMP) of fluorescent probes (Wade *et al.*, 1986; Dakin *et al.*, 2005). In the present study, the approach selected to study astrocytic gap junctions in acute brain slices is dye coupling, measured after loading of single astrocytes with a patch pipette containing biocytin during whole-cell recordings. With the restriction that it concerns only biocytin-permeability, this approach establishes a map of the cellular network that is connected to the astrocyte loaded with the tracer. Thus, the shape and extent of such communicating networks in different locations in brain structures and after pharmacological treatments can be compared, providing additional information on their functional organization and regulation properties. Although this approach is not dynamic and does not allow on-line analysis, such assessment of gap junction status gives anatomical information about functional networks.

### Cellular domain and network organization of astrocytes

Recently, the view of the spatial organization of a grey matter astrocyte has changed greatly and new concepts about their structural features have emerged at the single-cell level. Structural analysis performed on either living or fixed astrocytes labeled with fluorescent dyes (Grosche *et al.*, 1999; Bushong *et al.*, 2002; Bushong *et al.*, 2004) and astrocytes expressing EGFP under the control of the GFAP promoter (Nolte *et al.*, 2001; Hirrlinger *et al.*, 2004) demonstrates that astrocyte morphology cannot be reduced to the GFAP cytoskeleton visualized by immunostaining. Although cellular heterogeneity and developmental changes are parameters to keep in mind, an astrocyte is now described as a highly ramified cell with numerous processes that confer a ‘spongiform’ aspect rather than stellate, as reported classically. Interestingly these processes are highly dynamic because they exhibit a great motility, like dendritic spines in neurons, which indicates that the morphology of astrocytes is not fixed but is plastic (Hirrlinger *et al.*, 2004). Moreover, when spatial interactions between astrocytes are analyzed by 3D confocal microscopy, it appears that these

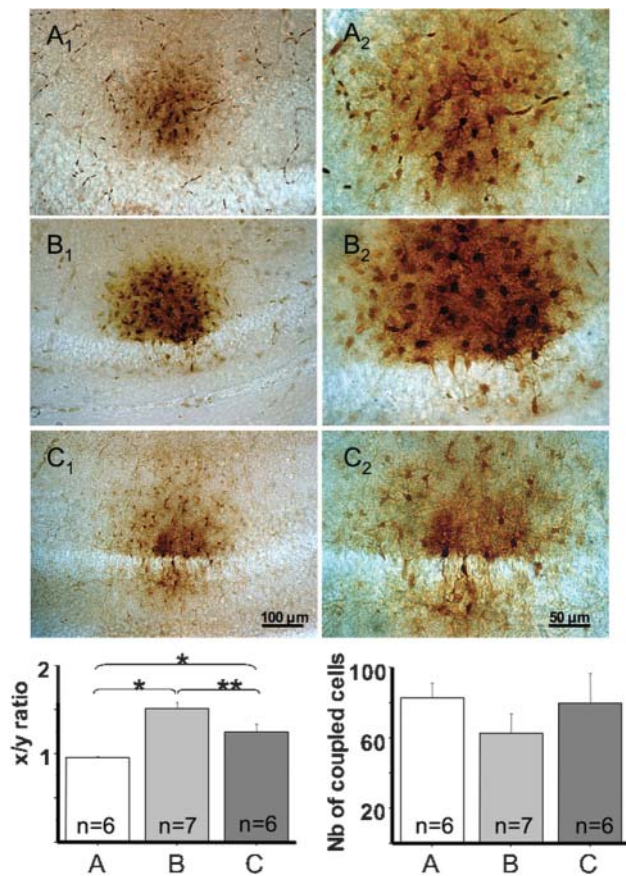


**Fig. 5. Astrocytic networks and intercellular diffusion of biocytin in the CA1 region of the hippocampus.** (A<sub>1</sub>,A<sub>2</sub>) Biocytin-loading of an astrocyte in the center of stratum radiatum, recorded under whole-cell condition, results in intercellular diffusion of the tracer that stains surrounding cells within a circular area. (B<sub>1</sub>-C<sub>2</sub>) When injections are made into an astrocyte in stratum radiatum but close to the pyramidal cell body layer (<50 μm), two types of network shapes are distinguished: either biocytin diffusion stopped in the pyramidal neuronal layer (B<sub>1</sub>,B<sub>2</sub>) or it stains astrocytes from stratum oriens (C<sub>1</sub>,C<sub>2</sub>). Quantification of the x:y ratio (x and y axes being defined as parallel and perpendicular to the pyramidal layer) is statistically different in these three conditions (left-hand diagram) but there is no statistical difference in the number of coupled cells (right-hand diagram).

cells define cellular domains that are not ‘inter-digitating’ as thought initially (Rohlfmann and Wolff, 1998). Indeed, they barely overlap and share only small areas of contact (Ogata and Kosaka, 2002; Nedergaard *et al.*, 2003; Volterra and Meldolesi, 2005). These observations indicate that each astrocyte covers a specific territory (Bushong *et al.*, 2002; Bushong *et al.*, 2004), as described for the dendritic field of some neurons. However, these new concepts do not integrate the fact that there are gap junctions at their contact areas and that, although astrocytes are anatomically rather independent, they are connected functionally and form a functional network (Giaume and McCarthy, 1996). Consequently, in addition to individual astrocytic domains, a second level of cellular organization, i.e. multicellular networks, must also be considered.

In the present study, we show that such networks do not include all EGFP-positive cells present in a defined area because some of the cells that lack dye coupling are intercalated within the communicating network (Fig. 7). This is in agreement with the recent demonstration that there are at least two

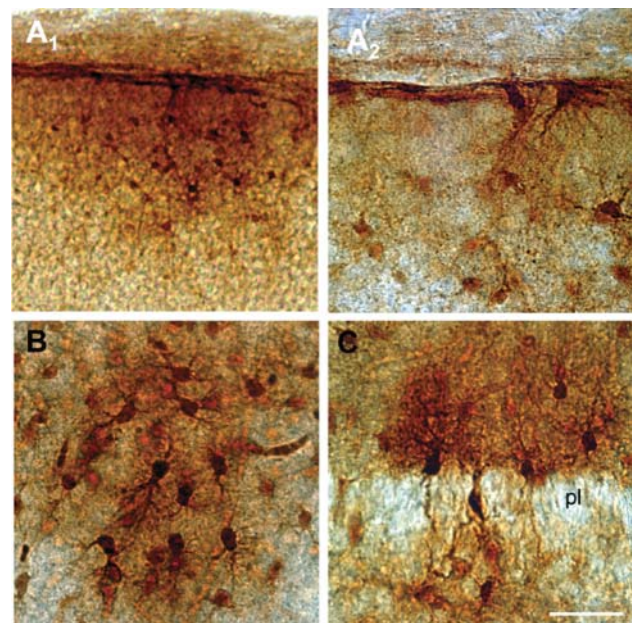


**Fig. 6. Morphological features of coupled cells in astrocytic networks in cortical and hippocampal slices.** (A<sub>1</sub>,A<sub>2</sub>) Biocytin injection by whole-cell recording of a cell identified as an astrocyte by its ‘passive’ electrophysiological properties followed by diffusion in layer I. At higher magnification (A<sub>2</sub>), the receiving cells have a morphology typical of astrocytes and are also detected in the superior part of layer I in cells identified as constituting the glia limitans, based on the elongated morphology running parallel to the surface of the cortex. (B,C) Two examples of an astrocytic network revealed by intercellular diffusion of biocytin following injections performed either in the center of the stratum radiatum (B) or in the close vicinity of the pyramidal cells layer (pl) (C). All stained cells have morphology typical of astrocytes and those that intercalate in the neuronal layer have an elongated feature similar to that observed with GFAP staining (Fig. 2B). Scale bar: 80 μm in A<sub>1</sub>; 30 μm in A<sub>2</sub>, B and C.

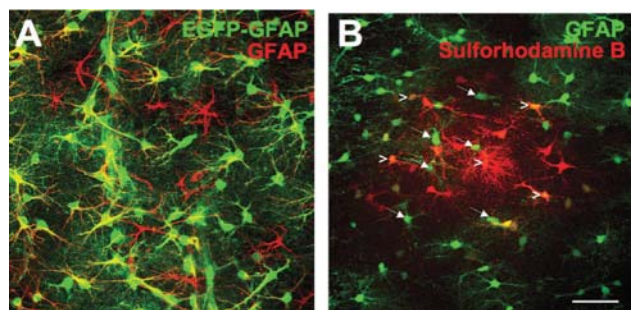


**Fig. 7. Confocal analysis of a subpopulation of GFAP-EGFP astrocytes and dye coupling in the hippocampus.** (A) EGFP and immunostaining for GFAP does not overlap totally in stratum radiatum. (B) Whole-cell recording of an astrocyte with a patch pipette containing sulforhodamine B stains 21 cells, 15 of which are EGFP-positive (some of these are indicated by arrowheads). Note that at least eight EGFP-positive cells (some indicated by arrows) that are in a position to be coupled do not stain, which indicates the presence of a restricted network of astrocytes. Scale bar: 50 μm.

subpopulations of EGFP-positive cells (which are thought to belong to the astrocyte family because the GFAP promoter is activated) in the supraoptic nucleus and the hippocampus, one of which is not coupled by gap junctions (Israel *et al.*, 2003; Wallraff *et al.*, 2004). In addition, although there is no doubt that the cell loaded initially is an astrocyte, a crucial question

remains about the identity of the coupled cells that constitute the network. This issue is difficult to resolve because the immunoreactivity for the most specific, widely used astrocytic marker, GFAP, is only partial in mouse astrocytes, particularly in the cortex. Unfortunately, the use of GFAP–EGFP mice does not solve this because not all astrocytes are fluorescent in the cerebral areas analyzed in these animals (Nolte *et al.*, 2001) (Fig. 7). In the future, other astrocyte markers such as sulforhodamine 101 might be used (Nimmerjahn *et al.*, 2004; Tian *et al.*, 2005). Nevertheless, it is noteworthy that the proportion of cells that are positive for GFAP–EGFP and dye coupled for sulforhodamine B (~60%) in mouse hippocampus and cortex is in the range reported in an *in vivo* study in adult mice (52%) (Nimmerjahn *et al.*, 2004). In rats, more cells (~80%) are positive for biocytin and GFAP after astrocyte dye-loading of P11–19 hippocampal slices (Blomstrand *et al.*, 2004) and this proportion was even higher in a previous study in cortical slices (Konietzko and Muller, 1994). Indeed, GFAP immunoreactivity is higher in rat astrocytes than mouse astrocytes. In the present work, a detailed analysis of the morphology of the coupled cells, fully represented thanks to biocytin filling, indicates that most of them are astrocytes (Fig. 6). In addition, no coupled cell with morphology typical of either a neuron or an oligodendrocyte was observed. A similar conclusion was made in a previous study performed in rat cortical slices from 6–120-day-old animals (Binmoller and Muller, 1992). Accordingly, we assume that cellular networks mapped by the intercellular diffusion of biocytin are composed mainly of astrocytes. However, we cannot exclude that the lack of coupling in some EGFP-positive cells and the detection of dye in EGFP-negative cells might reflect more subtle cellular heterogeneity within glial lineages. This controversial question remains to be addressed in future studies.

### Pattern of Cx43 expression and shape of dye coupling in astrocyte networks

As reported by several groups, immunostaining studies at the light and electron microscopic levels show that Cx43 is expressed mainly in astrocytes (in addition to meningeal and ependymal cells) and is absent from oligodendrocytes and neurons (Nagy *et al.*, 2004). Its absence in neurons has been confirmed recently by *in situ* hybridization studies in developing (P7) and adult rats (Condorelli *et al.*, 2003) and in mouse brain using a lacZ reporter gene engineered to replace the coding region of Cx43 in selected cell types (Theis *et al.*, 2003). The pattern of Cx43 expression is not homogeneous between and within cerebral areas (Yamamoto *et al.*, 1990; Nadarajah *et al.*, 1996; Nadarajah *et al.*, 1997). This heterogeneity is also observed in the present work in the mouse brain structures examined (cortex and hippocampus) (Fig. 1), and correlates differentially with anatomical compartments defined by neuronal layers. In the hippocampus, Cx43 expression is low in the pyramidal layer and granule cell layer of the dentate gyrus where neuronal somata are located and the number of GFAP-positive cells is reduced. In the cortex there is no clear-cut correlation between the level of Cx43 expression and the density of neuronal somata. Indeed, Cx43 is enriched in layer I, which contains rare neuronal somata, but also in layer IV, where somata of pyramidal neurons are dense. This heterogeneous distribution of Cx43 at P11 is similar to that observed in the adult mouse brain (data not shown). In addition,

heterogeneous expression of Cx43 was also observed at high magnification between adjacent astrocytes, which reinforces the emerging concept of astrocytic sub-populations, as discussed above. This observation might also be explained by a difference in the developmental stage of neighboring astrocytes. However, such patchy distribution of Cx43 has been reported for the hippocampus (stratum radiatum) in the adult rat (Yamamoto *et al.*, 1990). The distribution of the immunoreactive puncta of Cx43 at the cellular level indicates that most of the proteins do not form intercellular gap junctions between neighboring astrocytes because contact areas are rather small and astrocytic domains have limited overlap. This indicates that, in addition to a cytoplasmic localization, Cx43 is likely to be expressed at membrane sites that do not contact other astrocytes. Accordingly, Cx43 might contribute to functions other than direct intercellular communication. At least two roles for these Cx43 channels can be proposed: they might serve as hemichannels that allow the uptake and/or release of small molecules (Hofer and Dermietzel, 1998; Bennett *et al.*, 2003; Ye *et al.*, 2003) but, in this case, only few must open in control conditions because no dye leakage was detected. Alternatively, Cx43 channels might form reflexive gap junctions between processes of a same astrocyte, as previously proposed (Rohmann and Wolff, 1998; Wolff *et al.*, 1998). If confirmed, such a mode of autologous communication fits with the concept of astrocytic domains because reflexive gap junctions should favor the communication between the processes of a same cell. This might have important consequences for the physiology and function of astrocytes because it might affect their electrophysiological properties and the size of autonomous signaling microdomains.

Dye-coupling experiments indicate that the 2D organization of astrocytic networks depends on the site of injection in the cortex and the hippocampus. This modifies the view of a functional syncytium with virtually no border, as proposed initially from ultrastructural and functional studies (Mugnaini, 1986; Konietzko and Muller, 1994). As the extent of dye coupling is important and overpasses in many cases the physical boundaries of neuronal compartments, so far there is no evidence for the existence of independent astrocytic networks. However, we observed that, depending on the cortical layer or the hippocampal region, the coupling area is not necessarily circular, as would be expected if coupling was governed solely by a passive diffusion rule through homogeneously distributed astrocytes. Indeed, in cortical layers I and II/III and in the vicinity of the hippocampal pyramidal cell body layer, dye coupling is not symmetrical in the two perpendicular axes. This indicates the existence of constraints that shape the communicating network although diffusion remains passive. The nature of the constraint factors is a question to address in the future. Several directions can already be proposed, including: (1) a difference in astrocyte distribution within brain structures that might result from boundaries drawn by the presence of neuronal somata defining anatomical layers. This is the case in the hippocampal pyramidal cell body layer where only few astrocytes are intercalated between the tightly organized neurons (see Figs 2 and 5); (2) different sub-populations of astrocytes that differ in gap junction coupling (Israel *et al.*, 2003; Wallraff *et al.*, 2004), thus, network shape might depend directly on the proportion and distribution of these populations at defined ages and locations. The developmental aspect is likely to be important because at P9–11 not

all astrocytes are mature and their full content in Cxs is not yet reached; (3) the expression of surface molecules such as interacting proteins and cell-adhesion molecules and proteoglycans (Hofer *et al.*, 1996; Spray *et al.*, 1987) that are not part of the gap junction channels themselves but are crucial for the establishment of functional channels; (4) local neuronal release of neurotransmitters or active molecules might participate in the modeling of astrocytic networks; (5) alternatively, the existence of heterotypic gap junction channels and charge selectivity in dye permeability between sub-populations of coupled astrocytes cannot be excluded.

Another important observation is that there is no direct relationship between the pattern of Cx43 expression, investigated by immunofluorescence in confocal microscopy and the extent and shape of astrocytic networks studied using dye-coupling. Indeed, in the cortex, whatever the location of the astrocyte loaded with the biocytin, the number of cells coupled does not change, while the expression of Cx43 differs between layers. However, the lack of a direct correlation between the detection of the protein and its functional state should be nuanced by the fact that even in regions in which Cx43 expression is lower (cortical layers II/III and V, pyramidal cell layer in the hippocampus), it is still significant and sufficient to support intercellular communication. In fact, functional membrane proteins form only a small proportion of the total proteins expressed by a cell. This feature, which is reported for other membrane proteins such as receptors and ionic channels (Beck *et al.*, 1999; Rouach *et al.*, 2005) is also true for Cx43 (Bukauskas *et al.*, 2000). Indeed, there are some reports in which a lack of correlation between the level of Cx43 expression, studied by immunoblotting and immunofluorescence, and the extent of dye-coupling in astrocytes is observed (Rouach *et al.*, 2000; Alirezaei *et al.*, 2002). Finally, it should be kept in mind that as most of Cx43 reactivity is located in a single astrocytic domain rather than between astrocytes, correlation between levels of expression and coupling is not straightforward.

## ACKNOWLEDGEMENTS

We thank A.M. Godeheu for excellent technical assistance and S. Mouret for software assistance. This work was supported by the Ministère de la Recherche through the Action Concertée Incitative (ACI) 'Neurosciences Intégratives et Computationnelles' and the ANR Jemne checkeur N° OS-JCJC 0073-01.

## REFERENCES

- Alirezaei M., Mordelet E., Rouach N., Nairn A.C., Glowinski J. and Premont J. (2002) Zinc-induced inhibition of protein synthesis and reduction of connexin-43 expression and intercellular communication in mouse cortical astrocytes. *European Journal of Neuroscience* 16, 1037–1044.
- Beck S., Kuhr J., Schutz V.V., Seydewitz H.H., Brandis M., Greger R. *et al.* (1999) Lack of correlation between CFTR expression, CFTR Cl<sup>-</sup> currents, amiloride sensitive Na<sup>+</sup> conductance, and cystic fibrosis phenotype. *Pediatric Pulmonology* 27, 251–259.
- Bennett, M.V., Contreras, J.E., Bukauskas, F.F. and Saez, J.C. (2003) New roles for astrocytes: gap junction hemichannels have something to communicate. *Trends in Neurosciences* 26, 610–617.
- Binnmoller F.J. and Muller C.M. (1992) Postnatal development of dye-coupling among astrocytes in rat visual cortex. *Glia* 6, 127–137.
- Blomstrand F., Venance L., Siren A.L., Ezan P., Hanse E., Glowinski J. *et al.* (2004) Endothelins regulate astrocyte gap junctions in rat hippocampal slices. *European Journal of Neuroscience* 19, 1005–1015.
- Bushong E.A., Martone M.E., Jones Y.Z. and Ellisman M.H. (2002) Protoplasmic astrocytes in CA1 stratum radiatum occupy separate anatomical domains. *Journal of Neuroscience* 22, 183–192.
- Bushong E.A., Martone M.E. and Ellisman M.H. (2004) Maturation of astrocyte morphology and the establishment of astrocyte domains during postnatal hippocampal development. *International Journal of Developmental Neuroscience* 22, 73–86.
- Bukauskas F.F., Jordan K., Bukauskiene A., Bennett M.V., Lampe P.D., Laird D.W. *et al.* (2000) Clustering of connexin 43-enhanced green fluorescent protein gap junction channels and functional coupling in living cells. *Proceedings of the National Academy of Sciences of the U.S.A.* 14, 2556–2561.
- Condorelli D.F., Trovato-Salinaro A., Mudo G., Mirone M.B. and Belluardo N. (2003) Cellular expression of connexins in the rat brain: neuronal localization, effects of kainate-induced seizures and expression in apoptotic neuronal cells. *European Journal of Neuroscience* 18, 1807–1827.
- Dakin K., Zhao Y. and Li W.H. (2005) LAMP, a new imaging assay of gap junctional communication unveils that Ca<sup>2+</sup> influx inhibits cell coupling. *Nature Methods* 2, 55–62.
- Faustmann P.M., Haase C.G., Romberg S., Hinkerohe D., Szlachta D., Smikalla D. *et al.* (2003) Microglia activation influences dye coupling and Cx43 expression of the astrocytic network. *Glia* 42, 101–108.
- Filippov M.A., Hormuzdi S.G., Fuchs E.C. and Monyer H. (2003) A reporter allele for investigating connexin 26 gene expression in the mouse brain. *European Journal of Neuroscience* 18, 3183–3192.
- Giaume C. and McCarthy K.D. (1996) Control of gap-junctional communication in astrocytic networks. *Trends in Neurosciences* 19, 319–325.
- Grass D., Pawlowski P.G., Hirrlinger J., Papadopoulos N., Richter D.W., Kirchhoff F. *et al.* (2004) Diversity of functional astroglial properties in the respiratory network. *Journal of Neuroscience* 24, 1358–1365.
- Grosche J., Matyash V., Moller T., Verkhratsky A., Reichenbach A. and Kettenmann H. (1999) Microdomains for neuron-glia interaction: parallel fiber signaling to Bergmann glial cells. *Nature Neuroscience* 2, 139–143.
- Haas B., Schipke C.G., Peters O., Sohl G., Willecke K. and Kettenmann H. (2005) Activity-dependent ATP-waves in the Mouse Neocortex are Independent from Astrocytic Calcium Waves. *Cerebral Cortex*, PMID, 15930372, Epub ahead of print
- Hinkerohe D., Smikalla D., Haghikia A., Heupel K., Haase C.G., Dermietzel R. *et al.* (2005) Effects of cytokines on microglial phenotypes and astroglial coupling in an inflammatory coculture model. *Glia* 52, 85–97
- Hirrlinger J., Hulsmann S. and Kirchhoff F. (2004) Astroglial processes show spontaneous motility at active synaptic terminals in situ. *European Journal of Neuroscience* 20, 2235–2239.
- Hofer A., Saez J.C., Chang C.C., Trosko J.E., Spray D.C. and Dermietzel R. (1996) C-erbB2/neu transfection induces gap junctional communication incompetence in glial cells. *Journal of Neuroscience* 16, 4311–4321.
- Hofer A. and Dermietzel R. (1998) Visualization and functional blocking of gap junction hemichannels (connexons) with antibodies against external loop domains in astrocytes. *Glia* 24, 141–154.
- Israel J.M., Schipke C.G., Ohlemeyer C., Theodosis D.T. and Kettenmann H. (2003) GABAA receptor-expressing astrocytes in the

- supraoptic nucleus lack glutamate uptake and receptor currents. *Glia* 44, 102–110.
- Konietzko U. and Muller C.M.** (1994) Astrocytic dye coupling in rat hippocampus: topography, developmental onset, and modulation by protein kinase C. *Hippocampus* 4, 297–306.
- Koulakoff A., Meme W., Calvo C.F., Ezan P., Rouach N. and Giaume C.** (2003) Neurons and brain macrophages regulate connexin expression in cultured astrocytes. *Cell Communication and Adhesion* 10, 407–411.
- Kressin K., Kuprijanova E., Jabs R., Seifert G. and Steinhauser C.** (1995) Developmental regulation of Na<sup>+</sup> and K<sup>+</sup> conductances in glial cells of mouse hippocampal brain slices. *Glia* 15, 173–187.
- Kunzelmann P., Schroder W., Traub O., Steinhauser C., Dermietzel R. and Willecke K.** (1999) Late onset and increasing expression of the gap junction protein connexin30 in adult murine brain and long-term cultured astrocytes. *Glia* 25, 111–119.
- Leybaert L. and Sanderson M.J.** (2001) Intercellular calcium signaling and flash photolysis of caged compounds. A sensitive method to evaluate gap junctional coupling. In Bruzzone, R. and Giaume, C. (eds) *Connexin Methods and Protocols*. Humana Press, pp. 407–430.
- Matthias K., Kirchhoff F., Seifert G., Huttmann K., Matyash M., Kettenmann H. et al.** (2003) Segregated expression of AMPA-type glutamate receptors and glutamate transporters defines distinct astrocyte populations in the mouse hippocampus. *Journal of Neuroscience* 23, 1750–1758.
- Mercier F. and Hatton G.I.** (2000) Immunocytochemical basis for a meningeo-glial network. *Journal of Comparative Neurology* 420, 445–465.
- Mugnaini E.** (1986) Cell junctions of astrocytes, ependymal and related cells in the mammal central nervous system, with emphasis on the hypothesis of a generalized syncytium of supporting cells. In Fedozoff, S. and Vernadakis, A. (eds) *Astrocytes*. Academic Press, pp. 329–371.
- Méda P.** (2001) Assaying the molecular permeability of connexin channels. In Bruzzone, R. and Giaume, C. (eds) *Connexin Methods and Protocols*. Humana Press, pp. 201–224.
- Nadarajah B., Thomaidou D., Evans W.H. and Parnavelas J.G.** (1996) Gap junctions in the adult cerebral cortex: regional differences in their distribution and cellular expression of connexins. *Journal of Comparative Neurology* 376, 326–342.
- Nadarajah B., Jones A.M., Evans W.H. and Parnavelas J.G.** (1997) Differential expression of connexins during neocortical development and neuronal circuit formation. *Journal of Neuroscience* 17, 3096–3111.
- Nagy J.I. and Rash J.E.** (2000) Connexins and gap junctions of astrocytes and oligodendrocytes in the CNS. *Brain Research Brain Research Reviews* 32, 29–44.
- Nagy J.I., Li X., Rempel J., Stelmack G., Patel D., Staines W.A. et al.** (2001) Connexin26 in adult rodent central nervous system: demonstration at astrocytic gap junctions and colocalization with connexin30 and connexin43. *Journal of Comparative Neurology* 441, 302–323.
- Nagy J.I., Dudek F.E. and Rash J.E.** (2004) Update on connexins and gap junctions in neurons and glia in the mammalian nervous system. *Brain Research Brain Research Reviews* 47, 191–215.
- Nakase T. and Naus C.C.** (2004) Gap junctions and neurological disorders of the central nervous system. *Biochimica et Biophysica Acta* 1662, 149–158.
- Nedergaard M., Ransom B. and Goldman S.A.** (2003) New roles for astrocytes: redefining the functional architecture of the brain. *Trends in Neurosciences* 26, 523–530.
- Nimmerjahn A., Kirchhoff F., Kerr J.N. and Helmchen F.** (2004) Sulforhodamine 101 as a specific marker of astroglia in the neocortex in vivo. *Nature Methods* 1, 31–37.
- Nolte C., Matyash M., Pivneva T., Schipke C.G., Ohlemeyer C., Hanisch U.K. et al.** (2001) GFAP promoter-controlled EGFP-expressing transgenic mice: a tool to visualize astrocytes and astrogliosis in living brain tissue. *Glia* 33, 72–86.
- Ogata K. and Kosaka T.** (2002) Structural and quantitative analysis of astrocytes in the mouse hippocampus. *Neuroscience* 113, 221–233.
- Ransom B.R., Behar T. and Nedergaard M.** (2003) New roles for astrocytes (start at last). *Trends in Neurosciences* 26, 520–522.
- Ransom B.R. and Ye Z.C.** (2005) Gap junctions and hemichannels. In Kettenmann, H. and Ransom, B.R. (eds) *Neuroglia* (2nd edition), Oxford University Press, pp. 177–189.
- Roerig B. and Feller M.B.** (2000) Neurotransmitters and gap junctions in developing neural circuits. *Brain Research Reviews* 32, 86–114.
- Rohlmann A. and Wolff J.R.** (1998) Subcellular topography and plasticity of gap junction distribution in astrocytes. In Spray, D.C. and Dermietzel, R. (eds) *Gap Junctions in the Nervous System*, R.G. Landes, pp. 175–192.
- Rouach N., Glowinski J. and Giaume C.** (2000) Activity-dependent neuronal control of gap-junctional communication in astrocytes. *Journal of Cell Biology* 149, 1513–1526.
- Rouach N., Avignone E., Meme W., Koulakoff A., Venance L., Blomstrand F. et al.** (2002a) Gap junctions and connexin expression in the normal and pathological central nervous system. *Biology of the Cell* 94, 457–475.
- Rouach N., Calvo C.F., Glowinski J. and Giaume C.** (2002b) Brain macrophages inhibit gap junctional communication and down-regulate connexin 43 expression in cultured astrocytes. *European Journal of Neuroscience* 15, 403–407.
- Rouach N., Byrd K., Petralia R.S., Elias G.M., Adesnik H., Tomita S. et al.** (2005) TARP gamma-8 controls hippocampal AMPA receptor number, distribution and synaptic plasticity. *Nature Neuroscience* 8, 1525–1533.
- Spray D.C., Fujita M., Saez J.C., Choi H., Watanabe T., Hertzberg E. et al.** (1987) Proteoglycans and glycosaminoglycans induce gap junction synthesis and function in primary liver cultures. *Journal of Cell Biology* 105, 541–551.
- Steinhauser C., Berger T., Frotscher M. and Kettenmann H.** (1992) Heterogeneity in the membrane current pattern of identified glial cells in the hippocampal slice. *European Journal of Neuroscience* 4, 472–484.
- Theis M., Sohl G., Speidel D., Kuhn R. and Willecke K.** (2003) Connexin43 is not expressed in principal cells of mouse cortex and hippocampus. *European Journal of Neuroscience* 18, 267–274.
- Theis M., Sohl G., Eiberger J. and Willecke K.** (2005) Emerging complexities in identity and function of glial connexins. *Trends in Neurosciences* 28, 188–195.
- Tian G.F., Azmi H., Takano T., Xu Q., Peng W., Lin J. et al.** (2005) An astrocytic basis of epilepsy. *Nature Medicine* 11, 973–981.
- Van Rijen H.V.M., Wilders R., Rook M.B. and Jongasma H.J.** (2001) Dual patch Clamp. In Bruzzone, R. and Giaume, C. (eds) *Connexin Methods and Protocols*. Humana Press, pp. 269–292.
- Venance L., Cordier J., Monge M., Zalc B., Glowinski J. and Giaume C.** (1995) Homotypic and heterotypic coupling mediated by gap junctions during glial cell differentiation in vitro. *European Journal of Neuroscience* 7, 451–461.
- Volterra A. and Meldolesi J.** (2005) Astrocytes, from brain glue to communication elements: the revolution continues. *Nature Reviews Neuroscience* 6, 626–640.
- Wade M.H., Trosko J.E. and Schindler M.** (1986) A fluorescence photobleaching assay of gap junction-mediated communication between human cells. *Science* 232, 525–528.

- Wallraff A., Odermatt B., Willecke K. and Steinhauser C.** (2004) Distinct types of astroglial cells in the hippocampus differ in gap junction coupling. *Glia* 48, 36–43.
- Walz W.** (2000) Controversy surrounding the existence of discrete functional classes of astrocytes in adult gray matter. *Glia* 31, 95–103.
- Wolff J.R., Stuke K., Missler M., Tytko H., Schwarz P., Rohlmann A. et al.** (1998) Autocellular coupling by gap junctions in cultured astrocytes: a new view on cellular autoregulation during process formation. *Glia* 24, 121–140.
- Yamamoto T., Ochalski A., Hertzberg E.L. and Nagy J.I.** (1990) On the organization of astrocytic gap junctions in rat brain as suggested by LM and EM immunohistochemistry of connexin43 expression. *Journal of Comparative Neurology* 302, 853–883.
- Ye Z.C., Wyeth M.S., Baltan-Tekkok S. and Ransom B.R.** (2003) Functional hemichannels in astrocytes: a novel mechanism of glutamate release. *Journal of Neuroscience* 23, 3588–3596.

## AUTHORS' ADDRESSES

- <sup>1</sup> INSERM U114, Collège de France  
11 place Marcelin Berthelot  
75005 Paris  
France
- <sup>2</sup> Abteilung Neurogenetik  
Max Planck Institut für Experimentelle Medizin  
Hermann-Rein Strasse 3  
37075 Göttingen  
Germany

## Please address correspondence to:

Dr. Christian Giaume  
INSERM U114, Collège de France  
11 place Marcelin Berthelot  
75005 Paris  
France  
phone: 33 1 44 27 12 22  
fax: 33 1 44 27 12 60  
email: christian.giaume@college-de-france.fr